Chemical Engineering Journal 468 (2023) 143646

Contents lists available at ScienceDirect

Chemical Engineering Journal

journal homepage: www.elsevier.com/locate/cej

Step-wise SO_2-feeding strategies for microalgae-based CO_2 fixation from flue gas and bioenergy production

Yun Huang [a,b,1], Jingwei Fu [a,b,1], Ao Xia [a,b], Xianqing Zhu [a,b], Xun Zhu [a,b], Qiang Liao [a,b,*]

[a] Key Laboratory of Low-grade Energy Utilization Technologies and Systems, Chongqing University, Ministry of Education, Chongqing 400044, China
[b] Institute of Engineering Thermophysics, School of Energy and Power Engineering, Chongqing University, Chongqing 400044, China

ARTICLE INFO

Keywords:
Chlorella vulgaris
SO_2-feeding strategy
Carbon capture
Bioenergy
Enzyme activity

ABSTRACT

Aiming at eliminating the negative effect of SO_2 on microalgae CO_2 fixation caused by inappropriate SO_2-feeding strategies, physiology-based step-wise SO_2-feeding strategies were proposed to enhance the bioenergy production of microalgae. The step-wise SO_2-feeding strategy (four-step gradient increase from 100 to 400 ppm followed by four-step gradient decrease from 400 to 100 ppm) successfully realized the gratifying proliferation of microalgae by maintaining a better activity of ribulose-1,5-bisphosphate carboxylase/oxygenase (Rubisco), total adenosine triphosphatase (Total ATPase), superoxide dismutase (SOD), and catalase (CAT) enzyme. Moreover, the step-wise SO_2-feeding strategy, which considered the microalgal tolerance to sulfur at different growth stages, reduced the accumulation rate of toxic S-compounds in the culture medium by 47.2% and ensured a favorable solution pH of around 7 without the addition of alkaline chemical reagents. Sulfur replenishment and utilization were well-matched ($SO_2 \rightarrow HSO_3^- + SO_3^{2-} \rightarrow SO_4^{2-} \rightarrow$ intracellular ammonia acid) under a step-wise SO_2-feeding strategy, contributing to a maximum microalgal biomass concentration of 3.26 g L^{-1}, a photosynthetic efficiency of 10.89 %, and biomass energy of 18.97 kJ, which was 85.2%, 185%, and 390% higher than the microalgae cells cultivated under 300 ppm SO_2, respectively. Moreover, an increment of 81.4% in CO_2 utilization efficiency was also achieved. Overall, this study provided an effective method for achieving microalgal carbon capture from industrial flue gas with high SO_2 concentrations.

1. Introduction

As a promising Biomass Carbon Capture and Storage (BECCS) technique, microalgae-based CO_2 bio-fixation has been widely used in carbon neutralization processes due to its impressive carbon capture and conversion capability [1–3]. Generally, 1.83 kg CO_2 can be fixed by 1 kg photoautotrophic algal cells due to their outstanding photosynthetic efficiency, which is 10–50 times higher than terrestrial plants [4,5]. Subsequently, the intracellular inorganic carbon can be converted into various organic compounds, such as lipids, proteins, and carbohydrates, which can be further used to produce food, feed, biofuels, and other high-value-added products [6–8].

Flue gas waste streams from coal-fired power plants are a major source of anthropogenic CO_2 emissions and exacerbate climate change [9]. Microalgae have been shown to successfully realize carbon capture from simulated or industrial flue gas with CO_2 concentrations of 10–20% (v/v) [10,11]. However, the SO_2 present in flue gas has been proven to be toxic to algae cells and to impede carbon fixation [12,13]. Specifically, the sulfurous acid (H_2SO_3) is formed by a hydration reaction immediately after the water-soluble SO_2 gas dissolves into the culture medium ($SO_2 + H_2O \rightleftharpoons H_2SO_3$). Whereafter, the occurrence of dissociation ($H_2SO_3 \rightleftharpoons HSO_3^- + H^+$, $HSO_3^- \rightleftharpoons SO_3^{2-} + H^+$) and oxidation ($SO_2 + H_2O + \frac{1}{2}O_2 \Rightarrow H_2SO_4 \Rightarrow 2H^+ + SO_4^{2-}$) reactions contributes to the accumulation of hydrogen (H^+), bisulfite (HSO_3^-), sulfite (SO_3^{2-}), and sulfate (SO_4^{2-}) ions [14]. Among them, the sulfate ions can be assimilated by the algal cells as a sulfur source for the synthesis of amino acids and S-containing thylakoid lipids while the bisulfite and hydrogen ions are responsible for the inhibition of cell growth [15,16]. As previously reported, microalgal growth could be promoted at a low SO_2 concentration of 70 ppm while excess sulfur supply at 300 ppm SO_2 led to a 58% and 30% decrease in biomass yield and CO_2 fixation rate, respectively. Moreover, the cultivation collapsed when the SO_2 concentration reached 400 ppm due to severe solution acidification and bisulfite accumulation. More specifically, SO_2 and its hydrates can easily

* Corresponding author at: Institute of Engineering Thermophysics, School of Energy and Power Engineering, Chongqing University, Chongqing 400044, China.
E-mail address: lqzx@cqu.edu.cn (Q. Liao).
[1] These authors contributed equally to this work and are considered co-first authors.

https://doi.org/10.1016/j.cej.2023.143646
Received 7 February 2023; Received in revised form 29 April 2023; Accepted 17 May 2023
Available online 22 May 2023

intensify the acidification of the culture medium due to their high solubility and dissociation ability in water. For instance, under continuous aeration with simulated flue gas containing 400 ppm SO_2 at 0.1 vvm, the pH of the culture medium decreases to below 3 within 24 h [17]. Under these circumstances, bisulfite accumulates, which has been shown to block microalgal growth and even cause cell death when the concentration of bisulfite exceeds 1 mM [16,18]. Besides, the highly oxidative substances (e.g., superoxide anions, hydroxyl radicals, and hydrogen peroxide) generated in the conversion of bisulfite to sulfate have been confirmed to cause cell membrane damage and chlorophyll bleaching [16,19]. SO_2 is known to directly affect CO_2 fixation in plants by inhibiting the Rubisco enzyme and mitochondrial ATP production [16]. However, previous studies on the toxicity of SO_2 on microalgae have remained limited to its effect on biomass production. The mechanism of its effect on photosynthetic processes (e.g., electron transport, enzyme activity, intracellular component accumulation, etc.) of microalgae is still lacking.

Up to now, many efforts have been made to overcome SO_2-induced toxicity and acidification, such as adding alkaline reagents like NaOH, KOH, or $CaCO_3$, etc. to maintain a suitable pH of the culture medium [18,20,21], increasing the initial inoculation biomass concentration [22], decreasing the input SO_2 concentration [23], and shortening the exposure time of algae cells to the SO_2-containing flue gas by intermittent aeration [24]. As reported by Lee et al., the pH of the culture medium could be maintained at about 7 using NaOH which contributed to the growth of *Chlorella* KR-1 under the SO_2 concentration of 250 ppm [20]. However, the addition of these chemicals gives rise to high ionic strength (e.g., Na^+) which is unfavorable for microalgal growth and also increases the complexity and cost of microalgal cultivation. Increasing the inoculum concentration of microalgae may result in accelerated nutrient consumption (e.g., nitrate, phosphate, etc.) in the early stages of cultivation, which may not achieve ideal culture performance. Reducing the input SO_2 concentration can alleviate the accumulation of bisulfite and sulfate and solution acidification, but directly adopting a low SO_2 concentration for microalgae cultivation increases the cost of desulfurization in power plants. Adopting intermittent aeration allows a higher input SO_2 concentration, but the solution mixing caused by intermittent aeration is poor compared to continuous aeration, which may result in cell sedimentation and thus limit the algal photosynthesis. Based on this, optimization of continuous SO_2-feeding strategies is urgently needed to ensure successful microalgal CO_2 sequestration from SO_2-containing flue gas.

Traditionally, microalgae cultivation is carried out using flue gas with a constant SO_2 concentration of 100–300 ppm [12]. Nevertheless, it is hard to obtain an ideal biomass yield and carbon fixation efficiency at an SO_2 concentration of above 100 ppm without any pH-controlling methods [25]. Normally, freshwater microalgae cells contain only about 0.15 to 1.96% (w/w) of sulfur indicating a low sulfur requirement [14]. Hence, providing a low concentration of SO_2 in the early stage of cultivation can maintain cell growth as the microalgae cells show weak tolerance to high SO_2 concentrations in the early stage of cultivation due to low cell density and viability [20]. Once the microalgae successfully survive the early adaptation period, their demand for sulfur increases with increased biomass yield, and better cell viability allows them to tolerate higher SO_2 concentrations and regulate the pH of the culture medium [26]. What is noteworthy is that microalgal tolerance to SO_2 gradually decreases in the late stage of cultivation when the cells enter the growth stagnation period [15]. Above all, ensuring that the supply of SO_2 matches the requirement and tolerance of microalgae to sulfur at different physiological stages can be a promising way to enhance microalgae growth under flue gas with high SO_2 concentration.

Chlorella vulgaris is considered one of the most promising microalgae species for CO_2 fixation from industrial flue gas due to its good adaptability to high CO_2 and SO_2 concentrations [17,27,28]. Aiming to develop an effective SO_2-feeding strategy to increase the biomass yield of *Chlorella vulgaris* FACHB-31 under the SO_2 concentration of above 100 ppm, four step-wise SO_2-feeding strategies namely four-step gradient increase (Strategy I), four-step gradient increase followed by four-step gradient decrease (Strategy II), and two-step gradient increase (Strategy III and IV) in SO_2 concentration were proposed in this study. A comprehensive investigation of the solution properties and cell physiological responses under the step-wise and constant SO_2-feeding strategies was conducted, including the solution pH, SO_4^{2-} accumulation, biomass yield, cell composition (e.g., chlorophyll, lipids, carbohydrates, proteins, etc.), chlorophyll fluorescence characteristics (e.g., maximum photosynthetic efficiency of photosystem II, photochemical quenching, non-photochemical quenching, and maximum potential relative electron transport rate), and enzyme activity (Rubisco, Total ATPase, SOD, and CAT). Moreover, the light-to-biomass conversion processes characterized by light and CO_2 utilization, microalgal biomass energy production, and photosynthetic efficiency were assessed as well.

2. Materials and methods

2.1. Microalgae strain and cultivation

Chlorella vulgaris FACHB-31 (*C. vulgaris*) obtained from the Freshwater Algae Culture Collection of Hydrobiology, Chinese Academy of Science (China) was adopted as the microalgae strain and cultured with modified BG11 medium [29]. Batch cultivation of *C. vulgaris* was conducted in bubble column PBRs with a culture volume of 300 mL described in the previous study [17]. The initial inoculation cell density was 0.042 g L^{-1} and the initial pH was adjusted to 7.0 ± 0.1 using 1 M HCl or NaOH. Mixed gases containing different SO_2 concentrations of 0, 100, 200, 300, 400 ppm, and 15% (v/v) CO_2 (balanced with N_2) were continuously fed into the photoreactors at a flow rate of 50 mL min^{-1} controlled by a mass flow meter (FL-802, Flowmethod, Shenzhen, China). The incident light intensity was controlled at 120 μmol m^{-2} s^{-1} using an irradiatometer probe (FZ-A, Photoelectric Instrument Factory of Beijing Normal University, China). The pH of microalgae suspension (i.e., the mixture of algal cells and culture medium) was daily monitored using a pH meter (FG2, Mettler-Toledo, Switzerland). All the cultivation experiments were operated in a phytotron with a constant temperature of 25 ± 1℃.

2.2. Analytical methods

2.2.1. Determination of algal growth characteristics

The biomass concentration, daily growth rate, and specific growth rate of *C. vulgaris* were determined according to Sun et al [29]. Specifically, 9 mL of microalgae suspension sample was daily collected and centrifuged at 8000 rpm for 10 min followed by washing twice with distilled water. The algae cells were then dried in an oven at 85 °C until a constant weight was obtained. The daily growth rate (*DGR*) and specific growth rate (μ) were then calculated as follows:

$$\mathrm{DGR}\ (\mathrm{gL^{-1}day^{-1}}) = \frac{\Delta C}{\Delta t} \tag{1}$$

$$\mu(\mathrm{day^{-1}}) = \frac{\ln C_n - \ln C_0}{\Delta t} \tag{2}$$

where ΔC(g L^{-1}) is the variation in biomass concentration, Δt(day) is the variation in time, C_n (g L^{-1}) is the biomass concentration at the end of the culture, and C_0 (g L^{-1}) is the initial biomass concentration.

The CO_2 fixation rate was calculated as follows [17]:

$$R_{CO_2} = C_C \cdot P \cdot \left(\frac{M_{CO_2}}{M_C}\right) \tag{3}$$

where R_{CO_2} is the average CO_2 fixation rate (g L^{-1} day^{-1}), C_C is the carbon content in algal cells (%), P is the average biomass productivity (g L^{-1} day^{-1}), M_{CO_2} is the relative molecular mass of CO_2 (g mol^{-1}), and

M_C is the relative atomic mass of C (g mol^{-1}).

The chlorophyll content was determined using a UV spectrophotometer (Persee TU-1901, China) after 5 mL samples were treated with 5 mL of 95% methanol and centrifuged at 8000 rpm for 5 min, which was then calculated as follows [30]:

$$\text{Chlorophyll content } (mgL^{-1}) = 17.32 \times A_{645} + 7.18 \times A_{663} \quad (4)$$

where A_{645} and A_{663} are the absorbances at 645 nm and 663 nm respectively.

The SO_4^{2-} concentration was analyzed by ion chromatography (ICS-5000, ThermoFisher, USA) equipped with an anion analytical column (4 × 250 mm, AS11-HC) and a self-regenerating suppressor (4 mm, ASRS 300) [17]. The CO_2 utilization efficiency (*Ec*) was calculated as follows [31]:

$$Ec = \frac{\Delta C/12}{\sum_{i=0}^{n} M_{CO_2}/44} \times 100\% \quad (5)$$

where M_{CO_2} (g) is the consumption of CO_2, 12 is the molecular weight of carbon (g mol^{-1}), 44 is the molecular weight of CO_2 (g mol^{-1}), and ΔC (g) is the content of carbon fixed by microalgae in the culture media, which can be calculated as follows:

$$\Delta C = \Delta X \times V \times C_b + \Delta DOC \quad (6)$$

where ΔX (g L^{-1}) is the change of the biomass concentration over a growth slope, V (L) is the culture volume, C_b (g g^{-1}) is the carbon content of microalgae, and ΔDOC (g) is the change of the total dissolved organic carbon in the culture medium over the growth slope. The growth inhibition ratio (*IR*) was defined to describe the inhibition of different SO_2-feeding strategies on microalgal growth, which can be calculated as follows [32]:

$$IR(\%) = (1 - \frac{W_T}{W_C}) \times 100\% \quad (7)$$

where W_T and W_C are the final biomass concentration of the test group and control group, respectively.

2.2.2. Measurement of lipid, carbohydrate, and protein content

The lipid content (L_c) was measured using methanol, chloroform, and sulfuric acid according to Liao et al [33]. Specifically, 0.1 g of dried microalgae biomass was ground to powder and then mixed with 4 mL of chloroform, 4 mL of methanol, and 0.2 mL of sulphuric acid in a digestion reactor, which was then sealed and heated in an oven at 60 °C for 8 h, followed by cooling to room temperature. The product was washed at least three times with distilled water and dried at 60 °C to constant weight. The dried lipids were then measured gravimetrically. The protein content (P_c) was measured using a Quick Start Bradford Protein Assay kit purchased from Bio-Rad Pacific Limited (The United States) according to Lin et al [34]. 2 mL of the microalgal suspension was collected and centrifuged at 8000 rpm for 10 min. The algal cells were then mixed with deionized water and disrupted using the ultrasonic disruption method. Afterward, 0.1 mL of the disrupted microalgae suspension and 5 mL of dye (Quick StartTM Bradford 1x Dye Reagent) were mixed in a 10 mL centrifuge tube for 20 min. The protein concentration was then measured using the spectrophotometer at an absorbance of 485 nm. The carbohydrate content (C_c) was measured using a phenol–sulfuric acid protocol described by Dubois et al [35]. 2 mL of the disrupted microalgae suspension, 50 μL phenol solution (90%, w/w), and 5 mL sulfuric acid were mixed in a 10 mL centrifuge tube for 30 min until the mixture was cooled to room temperature. The carbohydrate concentration was then measured using the spectrophotometer at an absorbance of 595 nm.

2.2.3. Calculation of energy conversion from light to biomass

The light energy utilization efficiency (*LUE*) of microalgae was calculated as follows [30]:

$$LUE = \frac{BE}{LE} \times 100\% \quad (8)$$

where *BE* and *LE* are the biomass and light energy (kJ), respectively, which can be calculated as follows:

$$BE = DCW \times C_c \times 15.7 + L_c \times 37.6 + P_c \times 16.7 \quad (9)$$

$$LE = \frac{P_l}{10000} \times t_l \times 3600kJ/(kW{\cdot}h) \quad (10)$$

where *DCW* is the dry cell weight (g), C_c is the carbohydrate content (%), L_c is the lipid content (%), *Pc* is the protein content (%), P_l is the power of light (W), and t_l is the illumination time (h).

The photosynthetic efficiency (*PE*) was calculated as follows [36]:

$$PE = \frac{(C_1 - C_0){\cdot}H_G{\cdot}V{\cdot}10^3}{E_{in}{\cdot}S{\cdot}(t_1 - t_0)} \times 100\% \quad (11)$$

where C_0 and C_1 are the biomass concentration (g L^{-1}) at the initial time t_0 (s) and the ultimate time t_1 (s) of the cultivation period, respectively. H_G is the enthalpy of the dry biomass of *C. vulgaris* (kJ g^{-1}). E_{in} is the areal light energy input during cultivation (W m^{-2}).

2.2.4. Measurement of chlorophyll fluorescence

Chlorophyll fluorescence parameters including maximum photosynthetic efficiency of photosystem II (F_v/F_m), photochemical quenching (*qP*), non-photochemical quenching (*NPQ*), and relative electron transport rate of photosystem II (*rETR*), were measured using a chlorophyll fluorescence meter (Aqua Pen-C AP-C 100, Photon Systems Instruments, Czech Republic) after 15 min of dark adaptation for each sample (2 mL). The maximum potential relative electron transport rate of photosystem II ($rETR_{max}$) was calculated from *rETR* through nonlinear curve fitting [37]. The *rETR* was calculated as follows [38]:

$$rETR = PAR \times Y(II) \times f_1 \times f_2 \quad (12)$$

where *PAR* is the photosynthetically active radiation (μmol m^{-2} s^{-1}), *Y* (II) is the actual photosynthetic efficiency of photosystem II, f_1 (assumed to be 0.84) and f_2 (assumed to be 0.50) are the ETR factors which refer to the proportion of light energy absorbed by photosystem II to the total incident PAR [39].

2.2.5. Measurement of enzyme activity

20 mL algal samples were centrifuged at 10000 rpm for 10 min at 4 °C and the algal pellets were re-suspended with pre-cooling phosphate buffer (pH 6.8) and sonicated (Medium 200 W, 3 s of sonication strokes with 10 s of intervals) for 10 min in an ice bath. The homogenate was centrifuged, and the supernatants were used for enzyme activity assays according to the user guides. The activity of catalase (CAT) and ribulose-1,5-bisphosphate carboxylase/oxygenase (Rubisco) were measured using the assay kits purchased from Beijing Solarbio Science & Technology Co., Ltd. (China). The activity of superoxide dismutase (SOD) and total adenosine triphosphatase (Total ATPase) were measured using the assay kits purchased from GENMED SCIENTIFICS INC. U.S.A.

3. Results and discussion

3.1. Assessment of microalgal growth under constant SO_2 concentrations

The growth curves of *C. vulgaris* under different constant SO_2 concentrations of 0, 100, 200, 300, and 400 ppm are depicted in Fig. 1a. The results indicate that *C. vulgaris* cultured under 15% CO_2 (control group) exhibited a rapid growth trend in the first five days, followed by growth stagnation in the last three days of the whole culture period owing to the diminishing nutrients and attenuated illumination [29]. The maximum biomass concentration of 3.06 g L^{-1} was reached on day 7. By

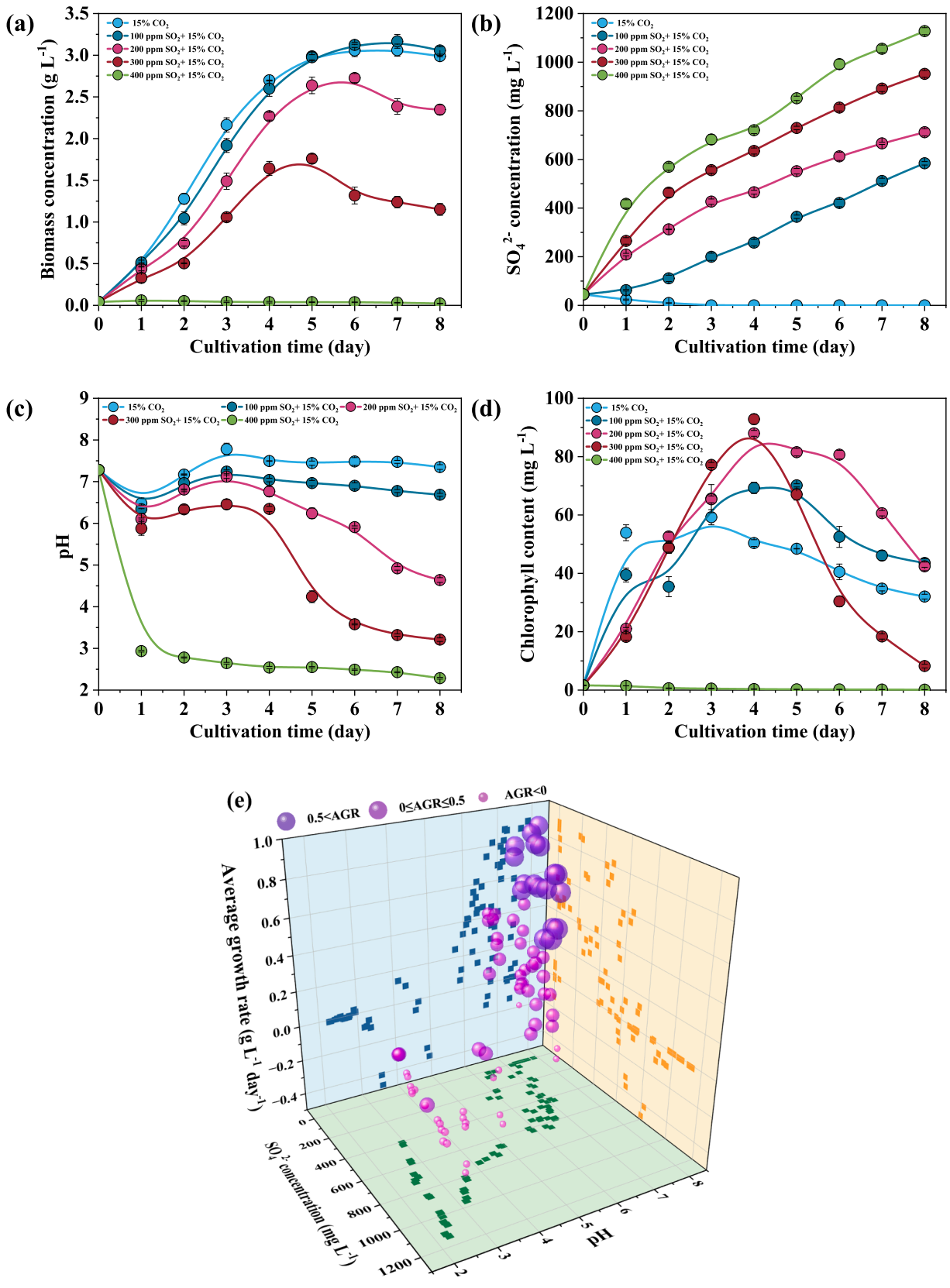

Fig. 1. Microalgal growth under constant SO_2 concentrations. (a) Biomass concentration, (b) SO_4^{2-} concentration, (c) pH of microalgae suspension, (d) Chlorophyll content, and (e) Average growth rate under different pH and SO_4^{2-} concentrations.

comparison, the growth status of *C. vulgaris* cultured at 15% CO_2 and 100 ppm SO_2 was slightly inhibited before day 5 but promoted afterward, accompanied by a maximum biomass concentration of 3.17 g L^{-1}. Unfortunately, the biomass yield of *C. vulgaris* showed an apparent decrease throughout the cultivation period when the SO_2 concentration increased to above 200 ppm. Specifically, compared to the control group (3.06 g L^{-1}), the maximum biomass concentration obtained under 200 ppm (2.73 g L^{-1}) and 300 ppm (1.76 g L^{-1}) decreased by 10.8% and 42.5%, respectively. In particular, *C. vulgaris* could not accumulate biomass under 400 ppm. The decrease in biomass yield was related to the sulfate accumulation and acidification of the solution. As shown in Fig. 1b, the sulfate concentration in the culture medium continuously increased in the test groups (100–400 ppm) but decreased in the control group (15% CO_2). Since sulfate can be utilized by microalgae cells as an S-source to maintain their basic physiological activities [15], the sulfate in the control group decreased from 45.3 to 0 mg L^{-1} in the first three days. The increase of sulfate in the test groups (100–400 ppm) was due to the continuous sparging with SO_2. After 8 days of cultivation, the sulfate concentration increased from 45.3 to 584.35 (100 ppm), 711.85 (200 ppm), 951.75 (300 ppm), and 1127.55 (400 ppm) mg L^{-1}, respectively. The accumulation of sulfate is because of the oxidation of bisulfite and sulfite, in which process the superoxide can be produced as well [16]. Bisulfite and superoxide are toxic to microalgae cells, especially in an acidic environment [19]. According to Fig. 1c, the pH of the control group (15% CO_2) and the test group (100 ppm) was maintained in the range of 6.3 and 7.5, which is preferred by *C. vulgaris* [40]. However, the pH of the culture medium decreased to 4.64 and 3.21 when SO_2 concentration increased to 200 and 300 ppm, respectively. In addition, the pH of the microalgae suspension decreased from 7.28 to 2.94 within 24 h when the SO_2 concentration increased to 400 ppm. The rapid acidification of the solution enhanced the toxicity of bisulfite to the algal cells, thereby inhibiting cell metabolism. Fig. 1d shows that the chlorophyll content of *C. vulgaris* firstly decreased with increased SO_2 concentrations in the first day. Generally, *C. vulgaris* exhibited low cellular activity and nutrients requirement in the adaptive phase and attempted to regulate the cell metabolism according to the environmental stimulus [40]. Lower solution pH and additional supplement of sulfate may inhibit the microalgal photosynthesis. In the middle stage of culture, the chlorophyll content increased with increased SO_2 concentration within 0–300 ppm while the chlorophyll was totally destroyed under 400 ppm SO_2. Sulfate is important for the synthesis of chlorophyll and related proteins in algal cells, and the chlorophyll content and sulfate concentration showed a positive correlation within a certain range of sulfate concentration [16,41]. In the later stage of culture, the excessive accumulation of sulfate, the acidification of solution, the lack of nutrients, and the decrease of algal cell activity occurred. The chlorophyll was either decomposed as an internal nitrogen source for cell growth or destroyed by the high concentration of sulfate, which resulted in the decrease of its content [17,42,43].

Fig. 1e shows the relationship between the average growth rate (AGR) of *C. vulgaris* and the sulfate concentration and pH. It can be concluded that *C. vulgaris* can maintain a high growth rate of more than 0.5 g L^{-1} day^{-1} when the sulfate concentration is 0 to 400 mg L^{-1}, and the pH is 6 to 8. In contrast, the growth of *C. vulgaris* can be inhibited when the sulfate concentration is more than 500 mg L^{-1} and the pH is lower than 5. The result is consistent with previous findings that the toxicity of S-compounds to microalgae cells can be enhanced in a lower pH of the culture medium [19]. Based on the above, the cultivation of *C. vulgaris*, fed with a constant SO_2 concentration above 300 ppm, is inappropriate because the SO_2 supply does not match the cell demand for sulfur. Hence, it may be possible to enhance the growth of *C. vulgaris* under high SO_2 concentration by changing the SO_2 concentration along with the physiological stages of *C. vulgaris* instead of keeping the SO_2 concentration constant throughout the cultivation cycle.

3.2. Responses of microalgal growth under step-wise SO_2-feeding strategies

Based on the results above, step-wise SO_2-feeding strategies I, II, III, and IV, namely four-step gradient increase (Strategy I) (Fig. 2a), four-step gradient increase followed by four-step gradient decrease (Strategy II) (Fig. 2b), and two-step gradient increase (Strategy III and IV) (Fig. 2c and 2d) in SO_2 concentration were adopted to investigate their influence on microalgal biomass production. The results in Fig. 2e indicate that the step-wise SO_2-feeding strategies enhanced *C. vulgaris* growth to different degrees compared with constant SO_2 concentrations of 100, 200, 300, and 400 ppm. Specifically, *C. vulgaris* cultured under the SO_2-feeding strategy II exhibited the best growth status with a maximum biomass concentration of 3.26 g L^{-1}, which was even better than the *C. vulgaris* cultured under a constant SO_2 concentration of 100 ppm (3.17 g L^{-1}). Interestingly, *C. vulgaris* cultured under the SO_2-feeding strategy III presented an unexpected growth trend. In other words, *C. vulgaris* successfully survived under 400 ppm SO_2 after being cultured with 100 ppm SO_2 for four days. Moreover, the maximum biomass concentration reached 2.95 g L^{-1}, which was only 3.59% lower than that achieved in the control group (3.06 g L^{-1}). The growth status of *C. vulgaris* cultured under the SO_2-feeding strategy I and IV was not desirable compared to SO_2-feeding strategies (II and III). However, the maximum biomass concentrations of SO_2-feeding strategy I (2.61 g L^{-1}) and IV (2.47 g L^{-1}) were slightly lower than that of 200 ppm (2.73 g L^{-1}) but higher than that of 300 ppm (1.76 g L^{-1}). Although the biomass yield under SO_2-feeding strategy I to IV has a clear difference, the step-wise SO_2-feeding strategies enhanced the growth of *C. vulgaris* under an SO_2 concentration of above 300 ppm. The explanation for these findings was that microalgae cells were sensitive to high SO_2 concentrations at lower cell densities (i.e., during the initial growth phase), and the sulfate requirement of microalgae cells was relatively lower in the meantime [26], so a lower SO_2 flux during the early cultivation process could not only guarantee sufficient sulfate for microalgal cells proliferation but also avoid the damage to the photosynthetic apparatus caused by S-induced toxicity resulting from high SO_2 concentration. Therefore, for SO_2-feeding strategies (I, II, and III), the lower SO_2 concentration during the initial cultivation days ensured a lower accumulation of S-compounds (Fig. 2f). Compared with the constant SO_2 concentrations of 200–400 ppm, the accumulation rate of SO_4^{2-} decreased by 10.03%-44.60% under SO_2-feeding strategy II. Furthermore, it was shown in Fig. 2g that the pH of the microalgae suspension was kept within 6–8 by adopting the step-wise SO_2-feeding strategy II and constant SO_2 concentrations of 0 and 100 ppm, which was preferred by the microalgal cells [40]. In contrast, the pH value showed different degrees of attenuation in the later stage of cultivation. Among them, the pH decrease under strategy I was the most severe, owing to the biomass decline from day 6 to day 8. As the culture proceeded, nutrient depletion, light attenuation, and cell senescence occurred [33], which limited the regulatory capacity and tolerance of microalgae cells to the environmental pH and toxic S-compounds. The chlorophyll content of *C. vulgaris* cultured under the step-wise SO_2-feeding strategy I to IV showed an upward tendency before day 5 and then decreased until day 8, similar to that of constant SO_2 concentrations of 0–300 ppm. The difference was that the step-wise SO_2-feeding strategy II to IV ensured a higher level of chlorophyll content in the later culture period (Fig. 2h). However, a sharp decrease of chlorophyll content was observed under the step-wise SO_2-feeding strategy I due to the death of algal cells caused by solution acidification and excessive accumulation of S-compounds.

3.3. Comparison of cell metabolism under constant and step-wise SO_2-feeding strategies

By adopting the step-wise SO_2-feeding strategy I, III, and constant SO_2-feeding strategies (0 and 100 ppm), one-third of the microalgal daily growth rates (DGRs) were above 0.5 g L^{-1} day^{-1} the other SO_2-

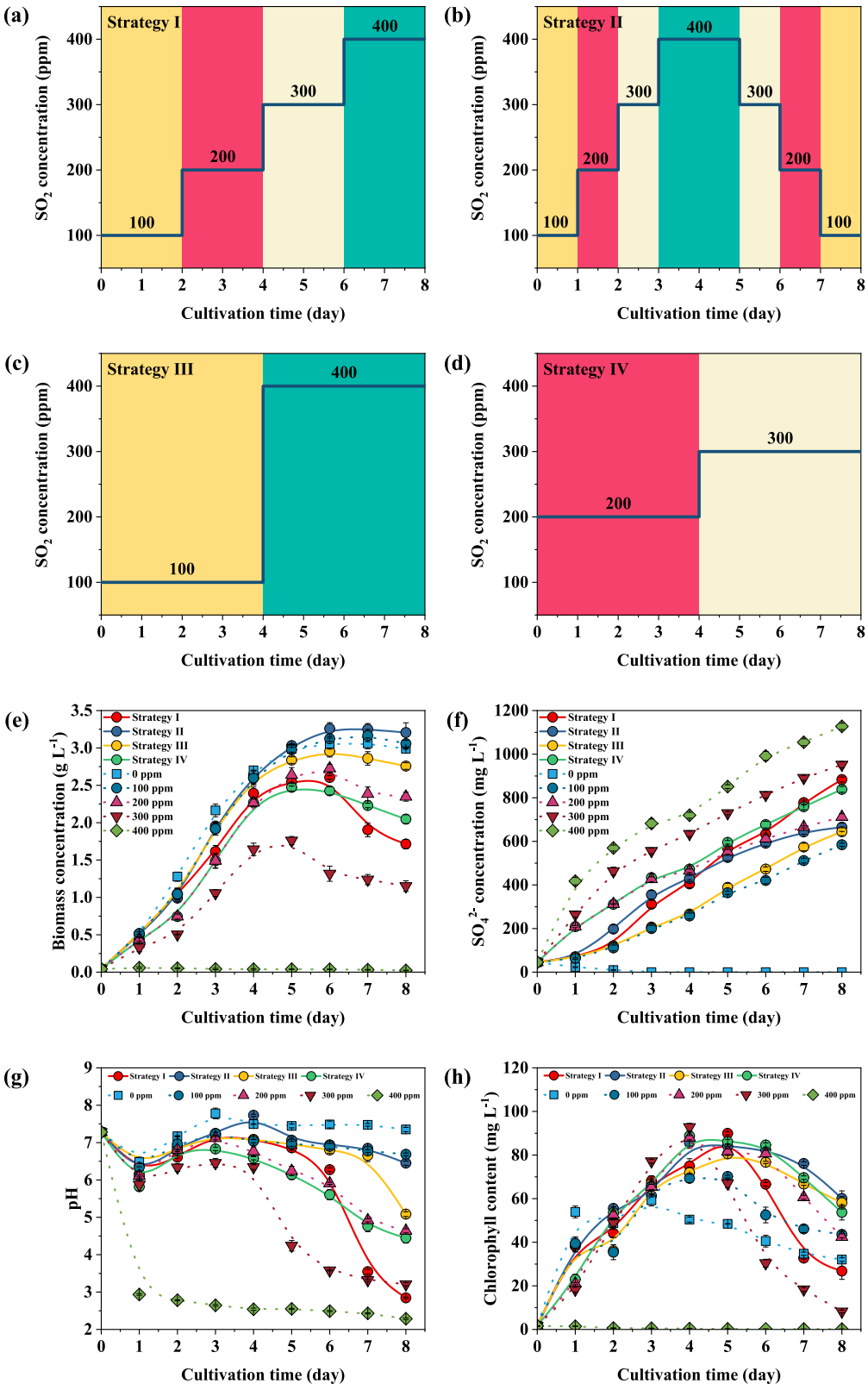

Fig. 2. Microalgal growth under step-wise SO_2-feeding strategies. (a) Strategy I, (b) Strategy II, (c) Strategy III, (d) Strategy IV, (e) Biomass concentration, (f) SO_4^{2-} concentration, (g) pH of microalgae suspension, and (h) Chlorophyll content.

feeding strategies contributed to 2/9 of the DGRs that were higher than 0.5 g L^{-1} day^{-1} (Fig. 3a). Moreover, 5/9 of the DGRs under step-wise SO_2-feeding strategy II and SO_2-feeding strategies (0–200 ppm) were in the range of 0 to 0.5 g L^{-1} day^{-1} while 4/9 of the DGRs under the other SO_2-feeding strategies were in the range of 0 to 0.5 g L^{-1} day^{-1}. Moreover, the average growth rate, average CO_2 fixation rate, and average specific growth rate throughout the culture period were also calculated (Fig. 3b). The results indicate that the step-wise SO_2-feeding strategy II

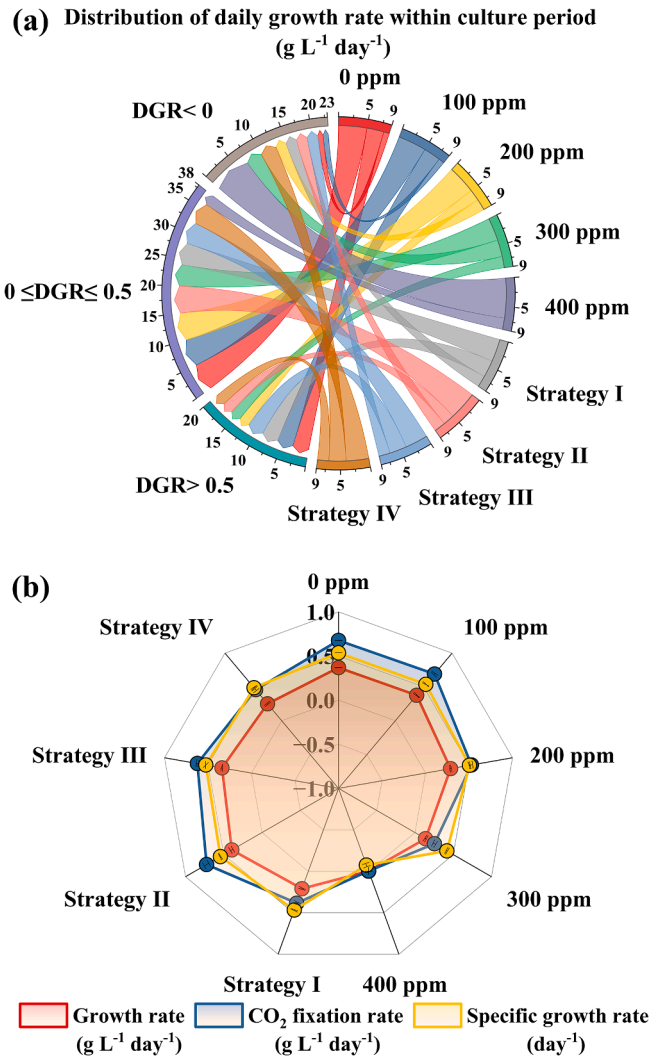

Fig. 3. Comparison of Microalgal growth and CO_2 fixation characteristics under different SO_2-feeding strategies. (a) Distribution of daily growth rate and (b) Average growth rate, CO_2 fixation rate, and specific growth rate.

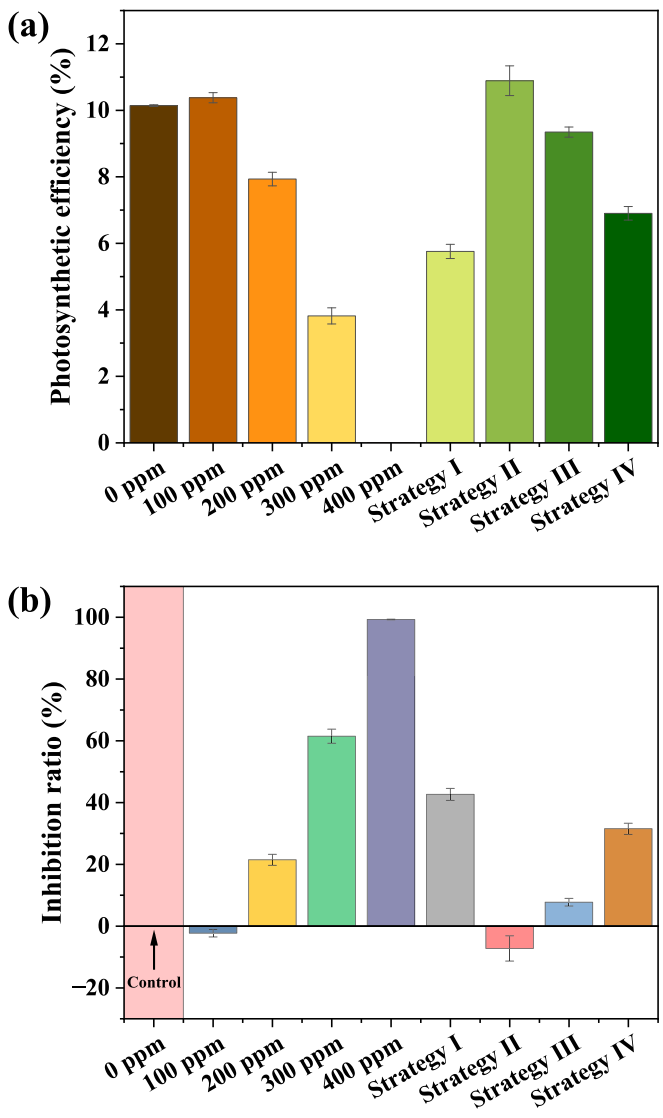

Fig. 4. (a) Photosynthetic efficiency and (b) Inhibition ratio under different SO_2-feeding strategies.

contributed to the highest average growth rate (0.40 g L^{-1} day^{-1}), average CO_2 fixation rate (0.73 g L^{-1} day^{-1}), and average specific growth rate (0.54 day^{-1}), which was 5.2%-186%, 5.8%-192%, and 0.92%-30.7% higher than that under constant SO_2-feeding strategies (0–300 ppm).

Fig. 4a shows the photosynthetic efficiency of *C. vulgaris* under different SO_2-feeding strategies. It was found that the step-wise SO_2-feeding strategy II also contributed to the highest photosynthetic efficiency of *C. vulgaris* (10.9%) due to the best growth status and highest biomass yield, indicating an improved light-to-biomass conversion efficiency. Under that circumstance, a promotion ratio of 7.27% was achieved under the step-wise SO_2-feeding strategy II compared to the control group (15% CO_2), while the constant SO_2-feeding strategies (200–400 ppm) resulted in the inhibition ratio up to 21%-99% (Fig. 4b).

The sulfate assimilated by algal cells is also used to produce various amino acids (e.g., cysteine and methionine), proteins (e.g., S-containing enzymes), S-containing thylakoid lipids, etc. [16]. Therefore, the total lipid, protein, and carbohydrate contents of *C. vulgaris* were evaluated as well (Fig. 5a). The results indicate that a similar level of lipid content (about 26%) was achieved under step-wise SO_2-feeding strategy II, III, and constant SO_2-feeding strategies (0–100 ppm) due to a similar growth status throughout the culture period. In contrast, the lipid content under the other SO_2-feeding strategies was within 14.5%-20.5%, indicating that adopting SO_2 concentrations above 200 ppm throughout the culture period was inappropriate for lipid accumulation. The highest protein content of *C. vulgaris* (47.8%) was achieved under step-wise SO_2-feeding strategy III, which was 0.84%-67% higher than the other SO_2-feeding strategies. The results show that the significant difference in SO_2 concentration provided by the early and late stages of the culture period (i.e., 100 ppm in the first four days and 400 ppm in the last four days) favored protein accumulation. In contrast, step-wise SO_2-feeding strategy II contributed to the highest carbohydrate content (14.0%), 6.1%-119% higher than the other SO_2-feeding strategies. The increase in carbohydrate accumulation revealed that the carbon assimilation by C. vulgaris was enhanced under the step-wise SO_2-feeding strategy II. The biomass energy of *C. vulgaris* was proportional to the content of the three major components (i.e., lipid, protein, and carbohydrate), contributing to the maximum biomass energy of 19.0 kJ under the step-wise SO_2-feeding strategy II, which was 8.6%-387% higher than the other SO_2-feeding strategies (Fig. 5b). A further comparison of the CO_2 and light energy utilization efficiencies were also conducted (Fig. 5b). The CO_2 and light energy utilization efficiencies were strongly related to the photosynthetic efficiency of *C. vulgaris*. As mentioned above, the step-wise SO_2-feeding strategy II contributed to the highest photosynthetic efficiency (Fig. 4a), and thus the maximum CO_2 utilization efficiency

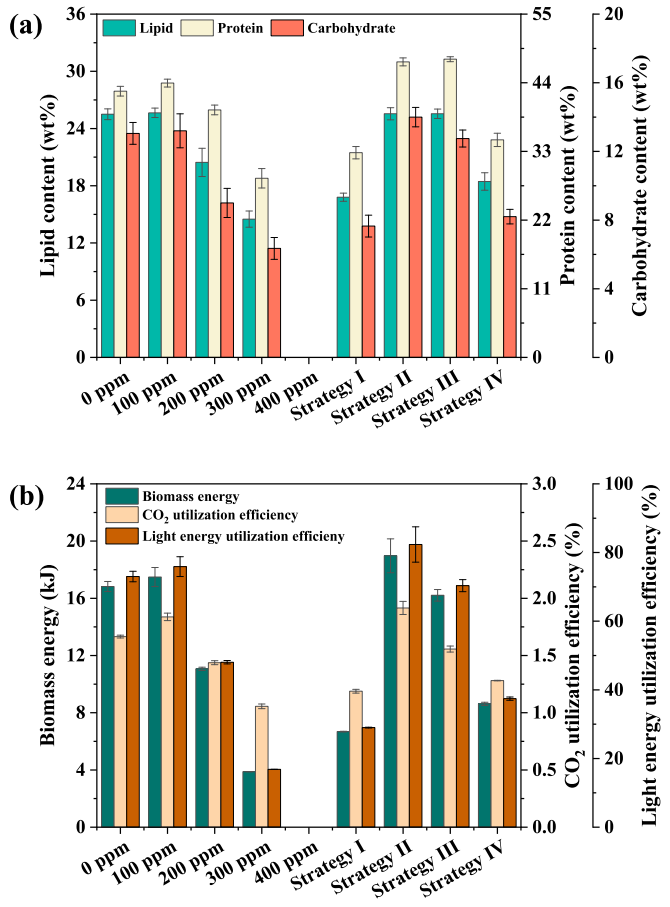

Fig. 5. Analysis of light-to-biomass conversion under different SO_2-feeding strategies. (a) Lipid, protein, and carbohydrate content, and (b) Biomass energy, CO_2, and light utilization efficiency.

(1.9%) and light energy utilization efficiency (82.3%) was achieved as well.

Chlorophyll fluorescence measurements are employed to gain insight into microalgal photosynthesis, which involves various interrelated biophysical and biochemical processes [44,45]. As shown in Fig. 6a, the photochemical quenching (qP) of *C. vulgaris* under different SO_2-feeding strategies showed an increasing trend at the beginning and then continuously decreased except for the *C. vulgaris* cultured under a constant SO_2 concentration of 400 ppm. Compared with the control group (15% CO_2), the *C. vulgaris* cultured under different SO_2-feeding strategies showed a decrease in photochemical quenching in the early culture period (before day 4), indicating the inhibition of S-compounds on cell photosynthesis. However, the photochemical quenching of *C. vulgaris* cultured with step-wise SO_2-feeding strategy II and constant SO_2 concentration of 100 ppm was higher than that of the control group (15% CO_2) in the later period of the culture process. It revealed that adopting a decreasing or low SO_2 concentration during the stable and declining phases of microalgal growth could promote the photosynthetic process since the excessive SO_2 input causes chlorophyll bleaching and photosystem destruction [17]. The non-photochemical quenching (NPQ) shown in Fig. 6b indicates that continuous feeding of SO_2 resulted in a decrease in the ability of algal cells to convert excess light intensity into heat. In other words, the ability of photoprotection was weakened. It should be noted, however, that non-photochemical quenching is related to the accumulation of carotenoids, which compete with chlorophyll production. A lower NPQ indicated that more light energy was captured and used for photosynthesis rather than being dissipated as heat [11]. As for the maximum potential relative electron transport rate of photosystem II ($rETR_{max}$), it can be concluded from Fig. 6c that the electron transport was hindered in the early stage of cultivation when SO_2 was applied, resulting in the inhibition of microalgal photosynthesis and biomass accumulation. However, the $rETR_{max}$ of *C. vulgaris* cultured with step-wise SO_2-feeding strategies was higher than that cultured with constant SO_2 concentrations above 100 ppm. In the late stage of cultivation, *C. vulgaris* cultured with step-wise SO_2-feeding strategy II to IV still showed an increase in the $rETR_{max}$ compared to that cultured with constant SO_2 concentrations above 200 ppm. A higher $rETR_{max}$ indicated higher photosynthetic efficiency and contributed an adequate flow of ATP and NADPH to the pathways required to fix inorganic carbon into organic skeletons for cell growth [46]. Therefore, a higher maximum light conversion efficiency of photosystem II (F_v/F_m) was achieved (Fig. 6d).

The enzyme activities shown in Fig. 7 were measured to investigate further the cellular metabolism of *C. vulgaris* under SO_2-feeding strategies. As shown in Fig. 7a and 7b, the SOD and CAT enzymes of the control group (15% CO_2) exhibited low activity and gradually decreased as the cultivation proceeded. The decrease in enzyme activity is related to the cell senescence as no SO_2-induced superoxides were formed. In comparison, the SOD and CAT enzyme activities of *C. vulgaris* cultured under step-wise SO_2 feeding and constant SO_2 concentration of 100 and 200 ppm increased from day 0 to day 4 and then decreased. However, the SOD and CAT enzyme activities decreased throughout the culture period when the constant SO_2 concentration increased to 300 ppm. Notably, the SOD and CAT enzymes were completely inactivated when the constant SO_2 concentration increased to 400 ppm. The results indicate that the SOD and CAT enzyme activity can be promoted under low SO_2 levels while inhibited under high SO_2 levels due to the formation of a large number of superoxides and acidification of the culture medium [16]. The Rubisco and total ATPase enzymes are essential for CO_2 fixation during photosynthesis. It can be concluded from Fig. 7c and 7d that the activity of Rubisco and Total ATPase enzymes in the control group (15% CO_2) was maintained at a high level but gradually inhibited as the constant SO_2 concentration increased, indicating that the Rubisco and Total ATPase enzymes can be inhibited by SO_2 at concentrations of 200 to 400 ppm. By contrast, there was no significant inhibitory effect of the step-wise SO_2-feeding strategy II, III, and low-SO_2-concentration feeding strategy (100 ppm) on Rubisco and total ATPase enzyme activities. The decrease in Rubisco and Total ATPase enzyme activities can directly limit or destroy microalgal photosynthesis.

3.4. Comparison of the maximum microalgal growth rates achieved via step-wise SO_2-feeding strategies with other regulation methods

Previous studies have reported several regulation methods to alleviate the SO_2-induced toxicity on microalgae, such as adding chemical reagents or buffers [10], increasing the initial inoculation biomass concentration [22], decreasing the input SO_2 concentration [23], and shortening the exposure time of algae cells to the SO_2-containing flue gas by adopting intermittent aeration strategy [24], etc. A comprehensive comparison of the maximum microalgal growth rate achieved by these methods and the step-wise SO_2-feeding strategies proposed in this study is shown in Table 1. To sustain the growth of *Desmodesmus* spp. in 100% unfiltered coal-fired flue gas with an SO_2 concentration of 270 ppm, Aslam et al. employed a 50 mM phosphate buffer (KH_2PO_4 & Na_2HPO_4) to stabilize the pH of the solution and gradually increased the flue gas concentration from 10% to 100%. A maximum growth rate of 0.045 g L^{-1} day^{-1} was acquired under 50% flue gas [10]. By increasing the inoculation concentration of microalgae cells, *Chlorella* sp. obtained a maximum growth rate of 0.52 g L^{-1} day^{-1} under the SO_2 concentration of 90 ppm [22]. However, increasing the inoculation concentration led to accelerated consumption of nutrients (e.g., nitrate, phosphate, etc.) in the early stage of cultivation, which may not achieve an ideal culture performance. Song et al. cultured the *Arthrospira* under continuous aeration with a low SO_2 concentration of 80 ppm, promoting biomass accumulation and a maximum growth rate of 0.65 g L^{-1} day^{-1} [23].

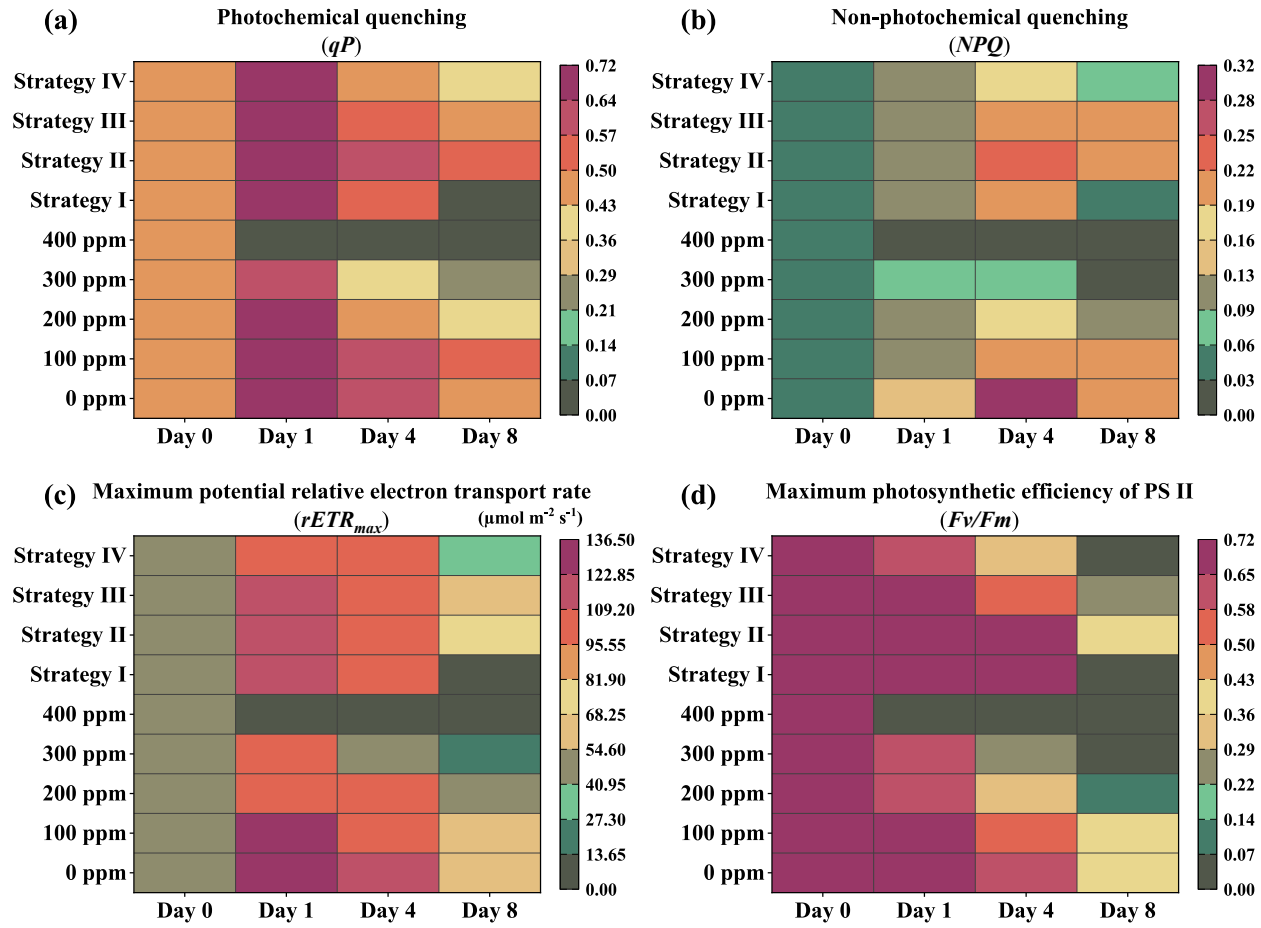

Fig. 6. Responses of photochemical efficiency under different SO_2-feeding strategies. (a) Photochemical quenching, (b) Non-photochemical quenching, (c) Maximum potential relative electron transport rate, and (d) Maximum photosynthetic efficiency of PSII.

What was worth mentioning was that the immediate adoption of low SO_2 concentration for microalgae cultivation might increase the cost of desulfurization in power plants. Intermittent aeration with a high SO_2 concentration of 400 ppm could be an alternative method, but the maximum growth rate (0.1 g L^{-1} day^{-1}) was unsatisfactory [24]. In this sense, the step-wise SO_2-feeding strategy proposed in this study could be a good choice, which ensured a maximum microalgal growth rate of 0.9645 g L^{-1} day^{-1} under an SO_2 concentration up to 400 ppm.

3.5. Practical application and perspectives on the future research

Compared with the constant SO_2-feeding strategy, the step-wise SO_2-feeding strategy could effectively alleviate the SO_2-induced toxicity on microalgae by slowing down the accumulation of S-compounds while maintaining the activity of algal photosynthetic enzymes (e.g., Rubisco, SOD, etc.), which allowed microalgae to thrive under SO_2 concentration up to 400 ppm. More importantly, the step-wise SO_2-feeding strategy increased the efficiency of CO_2 and light utilization and the synthesis of intracellular substances (e.g., proteins, carbohydrates, etc.) compared to a constant SO_2 concentration above 200 ppm. Therefore, the step-wise SO_2-feeding strategy was a promising method for efficient microalgae-based bio-decarbonization and bio-desulfurization from industrial flue gas. Moreover, from an economic perspective, the step-wise SO_2-feeding strategy was feasible to reduce the cost of desulfurization for a coal-fired power plant and the consumption of sulfur-containing nutrients, meanwhile ensuring sufficient algal biomass for further production of biofuels or high-value products.

For future research, the other beneficial or harmful substances in the flue gas (e.g., CO_2, NO_x, heavy metals, particulate matter, etc.) can also be regulated using the step-wise feeding strategy proposed in this study to enhance microalgal growth. However, it is worth noting that the requirement or tolerance of algal species to these substances at different growth stages should be investigated before applying the step-wise feeding strategy. Besides, the effect of light is still needed to be considered, as it is the driving force of photosynthesis and significantly impacts cell metabolism and CO_2 fixation [47]. Hence, a comprehensive kinetic model considering the synergistic effect of multi-factors (light, CO_2, SO_2, NO_x, heavy metals, and particulate matter, etc.) on microalgal growth is necessary to be established to provide a theoretical basis and optimization method for the step-wise feeding strategy.

4. Conclusions

The photosynthetic characteristics of *Chlorella vulgaris* FACHB-31 under four step-wise SO_2-feeding strategies were comprehensively evaluated and compared with those under constant SO_2-feeding strategies. The best growth status of *Chlorella vulagris* FACHB-31 was obtained under the step-wise SO_2-feeding strategy II (i.e., four-step gradient increase of SO_2 concentration from 100 to 400 ppm followed by four-step gradient decrease of SO_2 concentration from 400 to 100 ppm). By adopting the step-wise SO_2-feeding strategy II, the pH value of the culture medium was maintained in the favorable range of 6 and 8 throughout the culture period, and the accumulation rate of SO_4^{2-} decreased by 10.03%-44.60% compared with the constant SO_2 concentrations of 200–400 ppm, which ensured the better activity of SOD, CAT, Rubisco, and Total ATPase enzymes. In addition, the step-wise SO_2-feeding strategy II slowed down the decomposition of chlorophyll while contributing to the accumulation of proteins and carbohydrates in

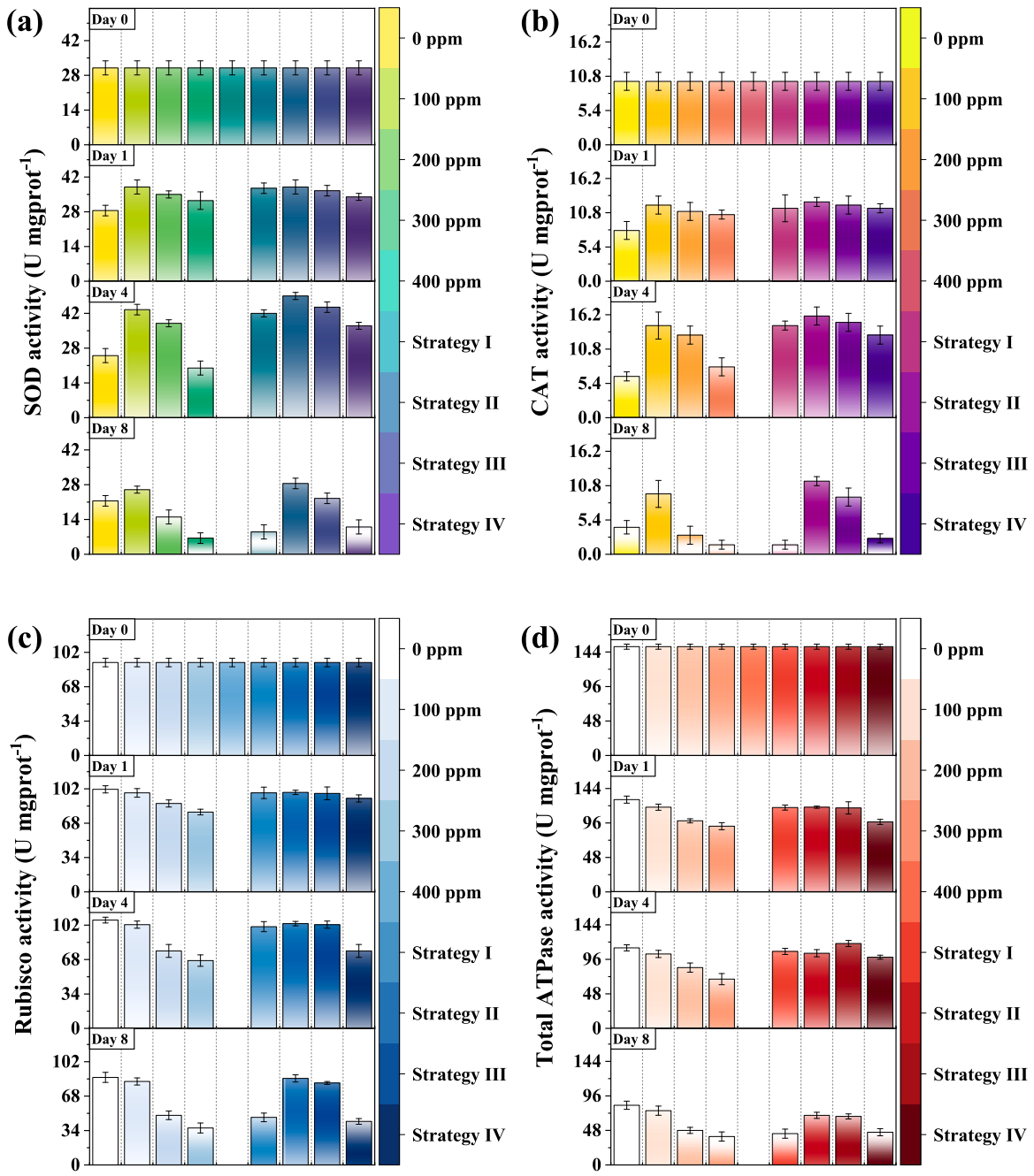

Fig. 7. Evaluation of enzyme activity under different SO_2-feeding strategies. (a) SOD activity, (b) CAT activity, (c) Rubisco activity, and (d) Total ATPase activity.

Table 1
Comparison of the algal growth rates under different regulation methods.

Regulation method	Microalgae species	CO_2 concentration (%)	SO_2 concentration (ppm)	Maximum growth rate (g L^{-1} day^{-1})	Ref.
Increasing inoculation concentration	*Chlorella* sp.	10	90	0.52	[22]
Intermittent SO_2-feeding strategy	*Chlorella fusca*	10	400	0.10	[24]
Adding chemical reagents/buffers	*Desmodesmus* spp.	11	270	0.045	[10]
Decreasing input SO_2 concentration	*Arthrospira*	15	80	0.65	[23]
Step-wise SO_2-feeding strategy	*Chlorella vulgaris*	15	100–400	0.96	This study

the later cultivation period. Compared with a constant SO_2 concentration of 200 ppm, an increase of 48.25% and 28.75% in the maximum potential electron transport rate and photochemical quenching was achieved under step-wise SO_2-feeding strategy II as well.

Declaration of Competing Interest

The authors declare that they have no known competing financial interests or personal relationships that could have appeared to influence the work reported in this paper.

Data availability

Data will be made available on request.

Acknowledgments

The authors are grateful for the financial support provided by the Innovative research group project of the National Natural Science Foundation of China (No. 52021004), the State Key Program of National Natural Science Foundation of China (No. 52236009), and the Fundamental Research Funds for the Central Universities (2022ZFJH004).

References

[1] W. Wu, L. Tan, H. Chang, C. Zhang, X. Tan, Q. Liao, N. Zhong, X. Zhang, Y. Zhang, S.-H. Ho, Advancements on process regulation for microalgae-based carbon neutrality and biodiesel production, Renew. Sust. Energ. Rev. 171 (2023), https://doi.org/10.1016/j.rser.2022.112969.

[2] S. Ma, W. Zeng, Y. Huang, X. Zhu, A.o. Xia, X. Zhu, Q. Liao, Revealing the synergistic effects of cells, pigments, and light spectra on light transfer during microalgae growth: a comprehensive light attenuation model, Bioresour. Technol. 348 (2022), https://doi.org/10.1016/j.biortech.2022.126777.

[3] W. Yang, S. Li, M. Qv, D. Dai, D. Liu, W. Wang, C. Tang, L. Zhu, Microalgal cultivation for the upgraded biogas by removing CO_2, coupled with the treatment of slurry from anaerobic digestion: A review, Bioresour. Technol. 364 (2022), 128118, https://doi.org/10.1016/j.biortech.2022.128118.

[4] W. Zhou, J. Wang, P. Chen, C. Ji, Q. Kang, B. Lu, K. Li, J. Liu, R. Ruan, Bio-mitigation of carbon dioxide using microalgal systems: Advances and perspectives, Renew. Sust. Energ. Rev. 76 (2017) 1163–1175, https://doi.org/10.1016/j.rser.2017.03.065.

[5] B.C. Klein, A. Bonomi, R. Maciel Filho, Integration of microalgae production with industrial biofuel facilities: a critical review, Renew, Sust. Energ. Rev. 82 (2018) 1376–1392, https://doi.org/10.1016/j.rser.2017.04.063.

[6] Y.A. Lim, M.N. Chong, S.C. Foo, I.M.S.K. Ilankoon, Analysis of direct and indirect quantification methods of CO_2 fixation via microalgae cultivation in photobioreactors: A critical review, Renew. Sust. Energ. Rev. 137 (2021), 110579, https://doi.org/10.1016/j.rser.2020.110579.

[7] Z. Ma, W.Y. Cheah, I.S. Ng, J.-S. Chang, M. Zhao, P.L. Show, Microalgae-based biotechnological sequestration of carbon dioxide for net zero emissions, Trends Biotechnol. 40 (12) (2022) 1439–1453, https://doi.org/10.1016/j.tibtech.2022.09.002.

[8] S. Ma, Y. Huang, B. Zhang, X. Zhu, A. Xia, X. Zhu, Q. Liao, Comprehensive modeling and predicting light transmission in microalgal biofilm, J. Environ. Manage. 326 (2023), 116757, https://doi.org/10.1016/j.jenvman.2022.116757.

[9] Z. Wang, J. Cheng, Y. Sun, D. Jia, Y. Tang, W. Yang, K. Cen, Comprehensive understanding of regulatory mechanisms, physiological models and key enzymes in microalgal cells based on various concentrations of CO_2, Chem. Eng. J. 454 (2023), 140233, https://doi.org/10.1016/j.cej.2022.140233.

[10] A. Aslam, S.R. Thomas-Hall, T.A. Mughal, P.M. Schenk, Selection and adaptation of microalgae to growth in 100% unfiltered coal-fired flue gas, Bioresour. Technol. 233 (2017) 271–283, https://doi.org/10.1016/j.biortech.2017.02.111.

[11] Z. Wang, J. Cheng, W. Song, X. Du, W. Yang, CO_2 gradient domestication produces gene mutation centered on cellular light response for efficient growth of microalgae in 15% CO_2 from flue gas, Chem. Eng. J. 429 (2022), 131968, https://doi.org/10.1016/j.cej.2021.131968.

[12] J.S. Lee, D.K. Kim, J.P. Lee, S.C. Park, J.H. Koh, H.S. Cho, S.W. Kim, Effects of SO_2 and NO on growth of *Chlorella* sp. KR-1, Bioresour. Technol. 82 (1) (2002) 1–4, https://doi.org/10.1016/s0960-8524(01)00158-4.

[13] S.R. Ronda, C. Kethineni, L.C.P. Parupudi, V.B.S.C. Thunuguntla, S. Vemula, V. S. Settaluri, P.R. Allu, S.K. Grande, S. Sharma, C.V. Kandala, A growth inhibitory model with SO_x influenced effective growth rate for estimation of algal biomass concentration under flue gas atmosphere, Bioresour. Technol. 152 (2014) 283–291, https://doi.org/10.1016/j.biortech.2013.10.091.

[14] C. Liu, Z. Zhao, L. Shao, L. Zhu, F. Xu, X. Jiang, C. Zheng, X. Gao, Experimental study and modified modeling on effect of SO_2 on CO_2 absorption using amine solution, Chem. Eng. J. 448 (2022), https://doi.org/10.1016/j.cej.2022.137751.

[15] H.R. Molitor, J.L. Schnoor, Using Simulated Flue Gas to Rapidly Grow Nutritious Microalgae with Enhanced Settleability, ACS Omega 5 (42) (2020) 27269–27277, https://doi.org/10.1021/acsomega.0c03492.

[16] S. Van den Hende, H. Vervaeren, N. Boon, Flue gas compounds and microalgae: (Bio-)chemical interactions leading to biotechnological opportunities, Biotechnol. Adv. 30 (6) (2012) 1405–1424, https://doi.org/10.1016/j.biotechadv.2012.02.015.

[17] J. Fu, Y. Huang, A. Xia, X. Zhu, X. Zhu, J.-S. Chang, Q. Liao, How the sulfur dioxide in the flue gas influence microalgal carbon dioxide fixation: From gas dissolution to cells growth, Renew, Energ. 198 (2022) 114–122, https://doi.org/10.1016/j.renene.2022.08.057.

[18] Y. Jiang, W. Zhang, J. Wang, Y. Chen, S. Shen, T. Liu, Utilization of simulated flue gas for cultivation of *Scenedesmus dimorphus*, Biorsour. Technol. 128 (2013) 359–364, https://doi.org/10.1016/j.biortech.2012.10.119.

[19] S.L. Yang, J. Wang, W. Cong, Z.L. Cai, O.Y. Fan, Effects of bisulfite and sulfite on the microalga *Botryococcus braunii*, Enzyme Microb. Tech. 35 (1) (2004) 46–50, https://doi.org/10.1016/j.enzmictec.2004.03.014.

[20] J.N. Lee, J.S. Lee, C.S. Shin, S.C. Park, S.W. Kim, Methods to enhance tolerances of *Chlorella* KR-1 to toxic compounds in flue gas, Appl. Biochem. Biotech. 84–6 (2000) 329–342, https://doi.org/10.1385/abab:84-86:1-9:329.

[21] Y.Y. Choi, J.M. Joun, J. Lee, M.E. Hong, P. Hoang-Minh, W.S. Chang, S.J. Sim, Development of large-scale and economic pH control system for outdoor cultivation of microalgae *Haematococcus pluvialis* using industrial flue gas, Bioresour. Technol. 244 (2017) 1235–1244, https://doi.org/10.1016/j.biortech.2017.05.147.

[22] S.-Y. Chiu, C.-Y. Kao, T.-T. Huang, C.-J. Lin, S.-C. Ong, C.-D. Chen, J.-S. Chang, C.-S. Lin, Microalgal biomass production and on-site bioremediation of carbon dioxide, nitrogen oxide and sulfur dioxide from flue gas using *Chlorella* sp. cultures, Bioresour. Technol. 102 (19) (2011) 9135–9142, https://doi.org/10.1016/j.biortech.2011.06.091.

[23] Y. Song, J. Cheng, Y. Miao, W. Guo, J. Zhou, SO_2 impurity in simulated flue gas with 15% CO_2 affects dynamic bubble dissolution and *Arthrospira* photosynthetic growth, ACS Sustain. Chem. Eng. 9 (16) (2021) 5580–5589, https://doi.org/10.1021/acssuschemeng.0c09197.

[24] J.H. Duarte, L.S. Fanka, J.A. Vieira Costa, Utilization of simulated flue gas containing CO_2, SO_2, NO and ash for *Chlorella fusca* cultivation, Bioresour. Technol. 214 (2016) 159–165, https://doi.org/10.1016/j.biortech.2016.04.078.

[25] H.-W. Yen, S.-H. Ho, C.-Y. Chen, J.-S. Chang, CO_2, NO_x and SO_x removal from flue gas via microalgae cultivation: A critical review, Biotechnol. J. 10 (6) (2015) 829–839, https://doi.org/10.1002/biot.201400707.

[26] D. Cheng, X. Li, Y. Yuan, C. Yang, T. Tang, Q. Zhao, Y. Sun, Adaptive evolution and carbon dioxide fixation of *Chlorella* sp. in simulated flue gas, Sci. Total Environ. 650 (2019) 2931–2938, https://doi.org/10.1016/j.scitotenv.2018.10.070.

[27] E. Daneshvar, R.J. Wicker, P.-L. Show, A. Bhatnagar, Biologically-mediated carbon capture and utilization by microalgae towards sustainable CO_2 biofixation and biomass valorization – A review, Chem. Eng. J. 427 (2022), 130884, https://doi.org/10.1016/j.cej.2021.130884.

[28] E.M. Valdovinos-García, J. Barajas-Fernández, M.d.L.Á. Olán-Acosta, M.A. Petriz-Prieto, A. Guzmán-López, M.G. Bravo-Sánchez, Techno-Economic Study of CO_2 Capture of a Thermoelectric Plant Using Microalgae (*Chlorella vulgaris*) for Production of Feedstock for Bioenergy, Energies 13 (2) (2020) 413.

[29] Y. Sun, Q. Liao, Y. Huang, A. Xia, Q. Fu, X. Zhu, J. Fu, J. Li, Application of growth-phase based light-feeding strategies to simultaneously enhance *Chlorella vulgaris* growth and lipid accumulation, Bioresour. Technol. 256 (2018) 421–430, https://doi.org/10.1016/j.biortech.2018.02.045.

[30] L. Yang, Q. Su, B. Si, Y. Zhang, Y. Zhang, H. Yang, X. Zhou, Enhancing bioenergy production with carbon capture of microalgae by ultraviolet spectrum conversion via graphene oxide quantum dots, Chem. Eng. J. 429 (2022), https://doi.org/10.1016/j.cej.2021.132230.

[31] Z. Sun, D. Zhang, C. Yan, W. Cong, Y. Lu, Promotion of microalgal biomass production and efficient use of CO_2 from flue gas by monoethanolamine, J. Chem. Technol. Biot. 90 (4) (2015) 730–738, https://doi.org/10.1002/jctb.4367.

[32] H. Li, Y. Zhang, J. Liu, Z. Shen, A. Li, T. Ma, Q. Feng, Y. Sun, Treatment of high-nitrate wastewater mixtures from MnO_2 industry by *Chlorella vulgaris*, Bioresour. Technol. 291 (2019), 121836, https://doi.org/10.1016/j.biortech.2019.121836.

[33] Q. Liao, Y. Sun, Y. Huang, A. Xia, Q. Fu, X. Zhu, Simultaneous enhancement of *Chlorella vulgaris* growth and lipid accumulation through the synergy effect between light and nitrate in a planar waveguide flat-plate photobioreactor, Bioresour. Technol. 243 (2017) 528–538, https://doi.org/10.1016/j.biortech.2017.06.091.

[34] K. Lin, A.o. Xia, Y. Huang, X. Zhu, K. Cai, Z. Wei, Q. Liao, Efficient production of sugar via continuous enzymatic hydrolysis in a microreactor loaded with cellulase, Chem. Eng. J. 445 (2022), https://doi.org/10.1016/j.cej.2022.136633.

[35] M. Dubois, K.A. Gilles, J.K. Hamilton, P.A. Rebers, F. Smith, Colorimetric method for determination of sugars and related substances, Anal. Chem. 28 (3) (1956) 350–356, https://doi.org/10.1021/ac60111a017.

[36] J. Fu, Y. Huang, Q. Liao, X. Zhu, A.o. Xia, X. Zhu, J.-S. Chang, Boosting photo-biochemical conversion and carbon dioxide bio-fixation of *Chlorella vulgaris* in an optimized photobioreactor with airfoil-shaped deflectors, Bioresour. Technol. 337 (2021), https://doi.org/10.1016/j.biortech.2021.125355.

[37] A.D. Jassby, T. Platt, Mathematical formulation of the relationship between photosynthesis and light for phytoplankton, Limnol. Oceanogr. 21 (4) (1976) 540–547, https://doi.org/10.4319/lo.1976.21.4.0540.

[38] B. Genty, J.M. Briantais, N.R. Baker, The relationship between the quantum yield of photosynthetic electron transport and quenching of chlorophyll fluorescence, Biochim. Biophys. Acta 990 (1) (1989) 87–92, https://doi.org/10.1016/s0304-4165(89)80016-9.

[39] J. Cheng, H. Lu, X. He, W. Yang, J. Zhou, K. Cen, Mutation of *Spirulina* sp. by nuclear irradiation to improve growth rate under 15% carbon dioxide in flue gas, Bioresour. Technol. 238 (2017) 650–656, https://doi.org/10.1016/j.biortech.2017.04.107.

[40] J. Fu, Y. Huang, Q. Liao, A. Xia, Q. Fu, X. Zhu, Photo-bioreactor design for microalgae: a review from the aspect of CO_2 transfer and conversion, Bioresour. Technol. 292 (2019) 121947, https://doi.org/10.1016/j.biortech.2019.121947.

[41] V. da Silva Ferreira, C. Sant'Anna, Impact of culture conditions on the chlorophyll content of microalgae for biotechnological applications, World J. Microb. Biot. 33 (1) (2016) 20, https://doi.org/10.1007/s11274-016-2181-6.

[42] Y. Huang, L. Luo, K. Xu, X.C. Wang, Characteristics of external carbon uptake by microalgae growth and associated effects on algal biomass composition, Bioresour. Technol. 292 (2019), 121887, https://doi.org/10.1016/j.biortech.2019.121887.

[43] G. Rosero-Chasoy, R.M. Rodríguez-Jasso, C.N. Aguilar, G. Buitrón, I. Chairez, H. A. Ruiz, Growth kinetics and quantification of carbohydrate, protein, lipids, and chlorophyll of *Spirulina platensis* under aqueous conditions using different carbon and nitrogen sources, Bioresour. Technol. 346 (2022), 126456, https://doi.org/10.1016/j.biortech.2021.126456.

[44] B. Tamburic, M. Szabó, N.-A.-T. Tran, A.W.D. Larkum, D.J. Suggett, P.J. Ralph, Action spectra of oxygen production and chlorophyll a fluorescence in the green microalga *Nannochloropsis oculata*, Bioresour. Technol. 169 (2014) 320–327, https://doi.org/10.1016/j.biortech.2014.07.008.

[45] A. Fratamico, P. Tocquin, F. Franck, The chlorophyll a fluorescence induction curve in the green microalga *Haematococcus pluvialis*: further insight into the nature of the P-S–M fluctuation and its relationship with the "low-wave" phenomenon at steady-state, Photosynth. Res. 128 (3) (2016) 271–285, https://doi.org/10.1007/s11120-016-0241-2.

[46] Z.-P. Ye, P. Robakowski, D.J. Suggett, A mechanistic model for the light response of photosynthetic electron transport rate based on light harvesting properties of photosynthetic pigment molecules, Planta 237 (3) (2013) 837–847, https://doi.org/10.1007/s00425-012-1790-z.

[47] Y. Ye, S. Ma, H. Peng, Y. Huang, W. Zeng, A. Xia, X. Zhu, Q. Liao, Insight into the comprehensive effect of carbon dioxide, light intensity and glucose on heterotrophic-assisted phototrophic microalgae biofilm growth: A multifactorial kinetic model, J. Environ. Manage. 325 (2023), 116582, https://doi.org/10.1016/j.jenvman.2022.116582.